Limitations of two-level emitters as nonlinearities in two-photon controlled-PHASE gates

Anders Nysteen,[1] Dara P. S. McCutcheon,[2] Mikkel Heuck,[3] Jesper Mørk,[1] and Dirk R. Englund[3]

[1]*DTU Fotonik, Department of Photonics Engineering, Technical University of Denmark, Building 343, 2800 Kgs. Lyngby, Denmark*

[2]*Quantum Engineering Technology Labs, H. H. Wills Physics Laboratory and Department of Electrical and Electronic Engineering, University of Bristol, Merchant Venturers Building, Woodland Road, Bristol BS8 1FD, United Kingdom*

[3]*Department of Electrical Engineering and Computer Science, Massachusetts Institute of Technology, Cambridge, Massachusetts 02139, USA*

(Received 14 December 2016; published 5 June 2017)

We investigate the origin of imperfections in the fidelity of a two-photon controlled-PHASE gate based on two-level-emitter nonlinearities. We focus on a passive system that operates without external modulations to enhance its performance. We demonstrate that the fidelity of the gate is limited by opposing requirements on the input pulse width for one- and two-photon-scattering events. For one-photon scattering, the spectral pulse width must be narrow compared with the emitter linewidth, while two-photon-scattering processes require the pulse width and emitter linewidth to be comparable. We find that these opposing requirements limit the maximum fidelity of the two-photon controlled-PHASE gate to 84% for photons with Gaussian spectral profiles.

DOI: 10.1103/PhysRevA.95.062304

I. INTRODUCTION

Key requirements for the successful implementation of photonic quantum computing architectures are (i) efficient sources of single indistinguishable photons, and (ii) a method to coherently interact two such photons [1–7]. Since these requirements were first stated, single-photon sources have steadily improved [7–10], with the most promising platforms based on few-level emitters, most notably semiconductor quantum dots [11–13] which now boast near-unity indistinguishability with (source to first objective) efficiencies above 70%. Generating photon-photon interactions can be achieved by "off-line nonlinearities" consisting of measurements and feed-forward [1–4,7], or deterministically by using "in-line" nonlinearities based on a nonlinear material through which two or more photons interact [14–17]. These in-line nonlinearities can in principle also be generated by few-level emitters [18–20], suggesting a quantum photonic architecture in which few-level systems act as both photon sources and photon couplers.

Experimentally, probabilistic photonic gates have been demonstrated by using off-line nonlinearities in both free space [7,21,22] and in integrated platforms [5,23]. Strong in-line nonlinearities and photon switching have been achieved by using Rubidium atoms strongly coupled to optical cavities [17,24–26], quantum dots in photonic crystal cavities [27–30], and nitrogen vacancy centers in diamond [31]. The potentially deterministic nature of few-photon in-line nonlinearities makes this approach particularly attractive for the realization of photonic gates, and a number of proposals have been put forward to construct controlled-PHASE gates on various platforms and with various degrees of complexity [14,15,32–36]. Some proposals even have the potential to operate at near-unity fidelities by using distributed interactions [36] or pulse reshaping techniques [35], although these approaches have the challenges of high complexity and potentially high losses. Ultimately the usefulness of a photonic gate in future quantum computing architectures will depend on the ease with which it can be experimentally realized and repeated, and the maximum efficiency and fidelity that it can achieve.

In this work we analyze the performance of perhaps the simplest deterministic passive controlled-PHASE gate, which acts on two uncorrelated indistinguishable photons in a dual-rail encoding. The idealized gate we consider uses the in-line nonlinearities of two two-level-emitters embedded in lossless waveguides. The fundamental operating principle of the gate relies on the saturability of a two-level emitter, which means that the phase imparted onto a photon or photons scattering on such an emitter depends on how many photons are present [19,20,37,38]. Although it has been shown that such a gate can never perform with perfect fidelity [38,39], the purpose of this work is to understand the limits and origins of its imperfections with a view towards improved future implementations. Even in the loss-less case where the gate is fully deterministic, we show that the maximum gate fidelity is limited to 84% for single photons with Gaussian spectral profiles. This number is determined by opposing requirements on the spectral width of the input photons; one-photon scattering requires spectrally narrow photons so that the greatest fraction is strictly resonant with the emitters, while two-photon scattering requires photons with spectral widths similar to the emitter linewidths, which maximizes saturation effects. Although the fidelities we calculate are significantly less than unity, in contrast to other schemes, the present one does not use dynamical photon capture methods [34], uses only two (identical) emitters per gate [36], and does not take advantage of possible pulse reshaping techniques [35], all of which are likely to introduce additional losses.

This paper is organized as follows: In Sec. II the basic gate structure and components are introduced, and the gate operation in an idealized case is discussed. In Secs. III and IV a more realistic scenario is analyzed and the linear and nonlinear gate operations are described. A general fidelity measure is considered in Sec. V to quantify the gate performance, and we conclude our findings in Sec. VI.

II. THE CONTROLLED-PHASE GATE

The structure implementing the gate, shown in Fig. 1, consists of two phase shifters, two directional couplers, and two two-level emitters, similar to the systems in Refs. [1,35,40]. We focus here on two-level-emitters, although we note that very-high-Q cavities could also be used [41,42], in which

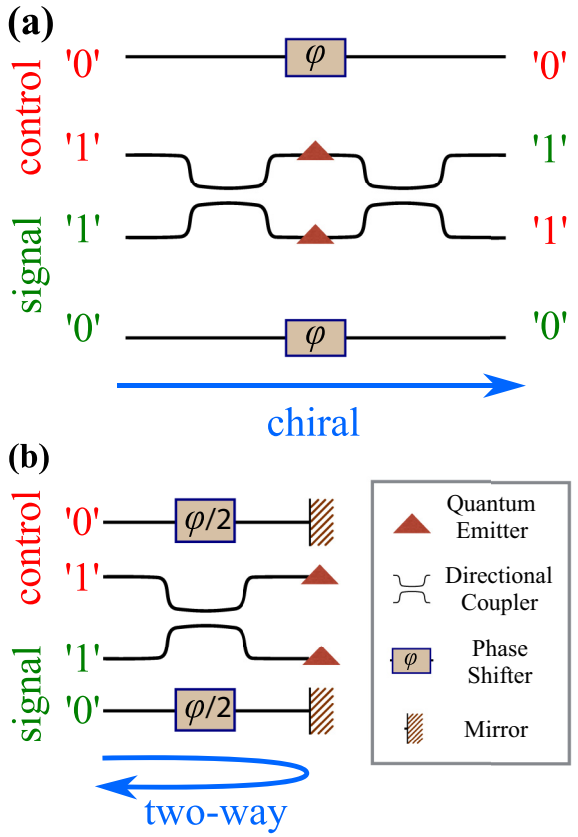

FIG. 1. (a) Schematic of the controlled-PHASE gate, which uses chiral waveguides, directional couplers, phase shifters, and two identical quantum emitters. The central idea of the gate is that the directional couplers act as 50/50 beam splitters, and as such the input state $|1_c\rangle|1_s\rangle$ gives rise to a Hong–Ou–Mandel bunching effect which can access the inherent nonlinearities of the emitters. Only the $|1_c\rangle|1_s\rangle$ input state bunches in this way, while all others transform linearly, thus providing a fundamental nonlinear interaction which can realize a two-photon gate. We focus on the chiral setup illustrated in panel (a), although an equivalent scheme can be realised with conventional bidirectional couplers as shown in panel (b). Note that the 1 arm for the control and signal is interchanged at the output ports in both cases.

splitting of the energy spectrum arises through the nonlinear Kerr effect [43]. In Fig. 1(a) we envisage chiral waveguides, for which propagation is permitted only in one direction. We note, however, that an equivalent scheme can be realized by using standard bidirectional waveguides with the emitters and perfectly reflecting mirrors placed at their ends, as illustrated in Fig. 1(b). For concreteness we focus on the chiral setup of Fig. 1(a), although all of our subsequent analysis equally applies to the two-way setup in Fig. 1(b). The central idea behind the scheme is that the components and waveguides are arranged in such a way that only the combined control and signal input state $|1_c\rangle|1_s\rangle$ accesses the nonlinearity of the two-level systems.

To gain some intuition, we first consider quasimonochromatic input photons, having a bandwidth much narrower than that of the emitters. Since the state of one photon can affect the state of the other, we must in general consider how pairs of photons are transformed by the gate components. Consider first the evolution of two photons in the state $|0_c\rangle|0_s\rangle$. From Fig. 1 we see that these photons each pick up a phase of φ, producing the transformation $|0_c\rangle|0_s\rangle \to e^{2i\varphi}|0_c\rangle|0_s\rangle$. For input states $|1_c\rangle|0_s\rangle$ or $|0_c\rangle|1_s\rangle$, the photon in the $|0\rangle$ state again picks up a phase of φ, while the other passes through the directional couplers and a two-level emitter. The directional couplers act as 50/50 beam splitters, affecting the mode transformation,

$$\begin{bmatrix} a_{1c}^\dagger \\ a_{1s}^\dagger \end{bmatrix} \longrightarrow \frac{1}{\sqrt{2}} \begin{bmatrix} 1 & -i \\ -i & 1 \end{bmatrix} \begin{bmatrix} a_{1c}^\dagger \\ a_{1s}^\dagger \end{bmatrix}, \tag{1}$$

where $a_{1c}^\dagger|\phi\rangle = |1_c\rangle$ and $a_{1s}^\dagger|\phi\rangle = |1_s\rangle$ with $|\phi\rangle$ denoting the vacuum. In this simplistic quasimonochromatic scenario, let us assume a single photon incident on the emitter acquires a phase of θ. Then the combined effects of the two directional couplers and the emitter cause the transformation $|1_s\rangle \to -ie^{i\theta}|1_c\rangle$ and $|1_c\rangle \to -ie^{i\theta}|1_s\rangle$. Therefore the photonic states transform as $|1_c\rangle|0_s\rangle \to -ie^{i\varphi}e^{i\theta}|1_s\rangle|0_s\rangle$ and $|0_c\rangle|1_s\rangle \to -ie^{i\varphi}e^{i\theta}|0_c\rangle|1_c\rangle$. Considering now the input state $|1_c\rangle|1_s\rangle$, we find that the action of the first directional coupler is to give rise to the Hong–Ou–Mandel interference effect; immediately after the first directional coupler we have a state proportional to $[(a_{1c}^\dagger)^2 + (a_{1s}^\dagger)^2]|\phi\rangle$, in which two photons are incident on each emitter in superposition. We denote the phase acquired by a two-photon state passing through an emitter as χ, and therefore find that, following the second directional coupler, we have the transformation $|1_c\rangle|1_s\rangle \to (-i)^2e^{i\chi}|1_c\rangle|1_s\rangle$.

Collecting these results and relabelling $-i|1_s\rangle \to |1_c\rangle$ and $-i|1_c\rangle \to |1_s\rangle$, we find

$$\begin{aligned} |0_c\rangle|0_s\rangle &\longrightarrow e^{2i\varphi}|0_c\rangle|0_s\rangle, \\ |0_c\rangle|1_s\rangle &\longrightarrow e^{i\varphi}e^{i\theta}|0_c\rangle|1_s\rangle, \\ |1_c\rangle|0_s\rangle &\longrightarrow e^{i\varphi}e^{i\theta}|1_c\rangle|0_s\rangle, \\ |1_c\rangle|1_s\rangle &\longrightarrow e^{i\chi}|1_c\rangle|1_s\rangle. \end{aligned} \tag{2}$$

If the emitters acted as linear optical elements, we would have $\chi = 2\theta$. Absorbing the phases φ and θ into the definitions of $|0\rangle$ and $|1\rangle$, respectively, the transformation is locally equivalent to the identity and therefore does not mediate any two-photon interaction. However, if the emitter-photon interaction can be tailored such that $\theta = \varphi$ and $\chi = 2\varphi + \pi$, the transformation in Eq. (2) becomes proportional to the desired control phase gate unitary diag$(1,1,1,-1)$. As such, if the conditions $\theta = \varphi$ and $\chi = 2\varphi + \pi$ can be met, a controlled-PHASE gate is realized. Although we do not expect this to be possible with perfect accuracy [38], in what follows we explore the differing requirements on the pulse shape relative to the emitter linewidth which these conditions impose.

In addition to the two-level-emitters, the other essential components of the gate are the directional couplers needed to produce the transformation in Eq. (1) and induce the Hong–Ou–Mandel effect for the input state $|1_c\rangle|1_s\rangle$. These components may be realized in various waveguide technologies, such as silica-on-silicon ridge waveguides [44], GaAs photonic ridge waveguide circuits [45], photonic-crystal waveguides [46], or silicon-on-insulator platforms [47], where in all cases the length of the coupling region must be engineered such the symmetrical beam splitter relation in Eq. (1) is achieved. We also note that, due to the choice of directional coupler, the

output port of the "1" control and signal states are swapped, as indicated in Fig. 1(a). This amounts to nothing more than notation and could easily be rectified by introducing a crossover between the two 1 outputs.

For proper functionality of the gate, the input states $|0_c\rangle|0_s\rangle$, $|1_c\rangle|0_s\rangle$, and $|0_c\rangle|1_s\rangle$, which only experience linear scattering effects, and the input state $|1_c\rangle|1_s\rangle$, which undergoes a nonlinear transformation, must all provide the desired output states in Eq. (2) when $\theta = \varphi$ and $\chi = 2\varphi + \pi$. These scattering-induced changes are investigated below, treating the linear and nonlinear case separately.

III. LINEAR GATE INTERACTIONS

Let us now consider the gate components in more detail and analyze the conditions under which the scheme can be realized for more realistic nonmonochromatic single-photon inputs. We describe a single photon in the $|0_c\rangle$ state as

$$|0_c\rangle = \int_{-\infty}^{\infty} dk\xi(k)a_{0c}^{\dagger}(k)|\phi\rangle, \tag{3}$$

where $|\phi\rangle$ is again the vacuum, $\xi(k)$ is the spectral profile of the photon satisfying $\int_{-\infty}^{\infty} dk|\xi(k)|^2 = 1$, while $a_{0c}^{\dagger}(k)$ is the creation operator of photons in the control "0" waveguide with momentum k, satisfying $[a_{0c}(k), a_{0c}^{\dagger}(k')] = \delta(k - k')$. We note that these conditions ensure that the input state $|0_c\rangle$ contains exactly one photon, and we consider a rotating frame such that k is measured relative to the carrier momentum, $k_0 = \omega_0/c$. The simple transformations in Eq. (2) are not generally valid for photonic wave packets comprised by many k modes because the phases φ and θ depend on k. In a large-scale system, the output from one gate must function as the input to another gate and they should therefore only differ by a time translation, which in momentum space corresponds to the transformation $\xi(k) \to \xi(k)e^{i\varphi(k)}$ with

$$\varphi(k) = \varphi_0 + kL, \tag{4}$$

where L is an additional optical path length of the 0 waveguides, either induced by a change in the refractive index of the material or by a longer arm length.

When $\varphi(k)$ is of the form in Eq. (4), the input state $|0_c\rangle|0_s\rangle$ is described by a product of two single-photon states of the form in Eq. (3), and we write the corresponding output state as $|0_c\rangle|0_s\rangle \to |\tilde{0}_c\rangle|\tilde{0}_s\rangle$ with

$$|\tilde{0}_c\rangle = -\int_{-\infty}^{\infty} dk\xi(k)e^{ikL}a_{0c}^{\dagger}(k)|\phi\rangle, \tag{5}$$

and a similar definition for $|\tilde{0}_s\rangle$. Single photons with states of this form will be considered our "ideal" output states, since they are identical to the input state up to a linear frequency-dependent phase corresponding to a fixed temporal delay. The choice of $\varphi_0 = \pi$ has been chosen in anticipation of the transformation of the $|0_c\rangle|1_s\rangle$ state discussed below.

We now consider changes to the two input states with a single photon in one of the 1 arms, $|0_c\rangle|1_s\rangle$ and $|1_c\rangle|0_s\rangle$. The photon in the 0 arm is treated analogously to Eq. (5), while that in the 1 arm instead interacts with an emitter. Photons passing through the 1 arms must also give rise to states differing from input states only by a time translation. To see the conditions under which this is the case, we consider a nonmonochromatic single photon as described by Eq. (3) scattering on a two-level emitter in a chiral waveguide. The photon will acquire a complex coefficient $t(k)$ for each momentum component k, resulting in a photon with spectral profile $t(k)\xi(k)$. The frequency-dependent transmission coefficient is [48,49]

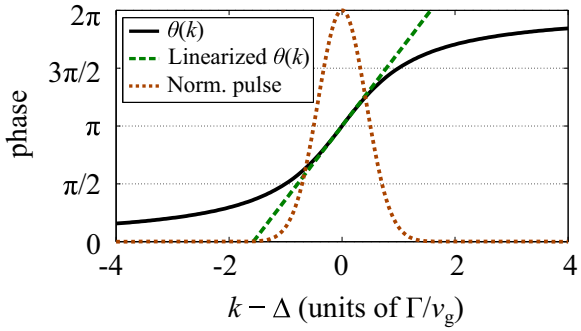

FIG. 2. Phase $\theta(k)$ acquired by a single-photon wave-packet component with moment k propagating in a chiral waveguide scattering on a lossless resonant emitter (black solid line), together with a linear approximation; see Eq. (8) (green dashed line). By comparison, the spectrum of a resonant Gaussian wave packet with spectral FWHM of $\sigma = \Gamma/v_g$ is shown (orange dotted line) with a scaled intensity to match the plotting window.

$$t(k) = \frac{k - \Delta - i(\Gamma - \gamma)/v_g}{k - \Delta + i(\Gamma + \gamma)/v_g}, \tag{6}$$

where v_g is the group velocity in the waveguide, Δ is the momentum detuning of the emitter from the pulse carrier frequency, Γ is the emitter decay rate into waveguide modes, and γ is the loss rate into modes outside the waveguide [49]. Recalling the effect of the directional couplers, we find that the states transform as $|0_c\rangle|1_s\rangle \to -i|\tilde{0}_c\rangle|\bar{1}_c\rangle$ and $|1_c\rangle|0_s\rangle \to -i|\bar{1}_s\rangle|\tilde{0}_s\rangle$, where

$$|\bar{1}_c\rangle = \int_{-\infty}^{\infty} dk\xi(k)t(k)a_{1c}^{\dagger}(k)|\phi\rangle, \tag{7}$$

with a similar definition for $|\bar{1}_s\rangle$. In the lossless case, $\gamma = 0$ and $|t(k)| = 1$, meaning that $\langle\bar{1}_c|\bar{1}_c\rangle = 1$ and the output state contains exactly one photon. As previously discussed, we can simply relabel what we refer to as the control and signal photons in the outputs and absorb factors of $-i$ in these definitions. We then have $|0_c\rangle|1_s\rangle \to |\tilde{0}_c\rangle|\bar{1}_s\rangle$ and $|1_c\rangle|0_s\rangle \to |\bar{1}_c\rangle|\tilde{0}_s\rangle$.

What is required, however, is that each photon has a spectral profile identical to an ideal state, $|\tilde{1}_c\rangle$ or $|\tilde{1}_s\rangle$, defined as in Eq. (5) with $a_{0c}^{\dagger}$ replaced with $a_{1c}^{\dagger}$ or $a_{1s}^{\dagger}$. Considering again the lossless case where $\gamma = 0$ we can write $t(k) = \exp[i\theta(k)]$. The phase $\theta(k)$ is shown as a function of k in Fig. 2. If the incoming single photon has a carrier frequency corresponding to the emitter transition frequency, $\Delta = 0$, the phase can be Taylor expanded around $k/\tilde{\Gamma} = 0$, producing

$$\theta(k) = \pi + 2\frac{k}{\tilde{\Gamma}} + O\left(\frac{k}{\tilde{\Gamma}}\right)^3, \tag{8}$$

where $\tilde{\Gamma} = \Gamma/v_g$. Keeping the condition $\varphi = \theta$ in mind and comparing Eqs. (4) and (8), we see that a good gate performance requires $|k| \ll \tilde{\Gamma}$, which corresponds to pulses with a spectrum that is much narrower than the emitter

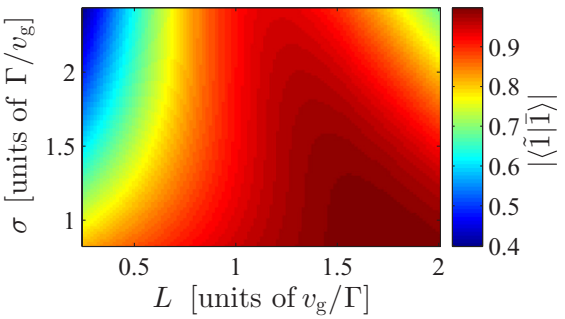

FIG. 3. Overlap between the ideal and scattered state for logical inputs $|1_c\rangle|0_s\rangle$ or $|0_c\rangle|1_s\rangle$ as a function of the additional optical length of the 0 arms, L, and the input spectral width σ defined in Eq. (9).

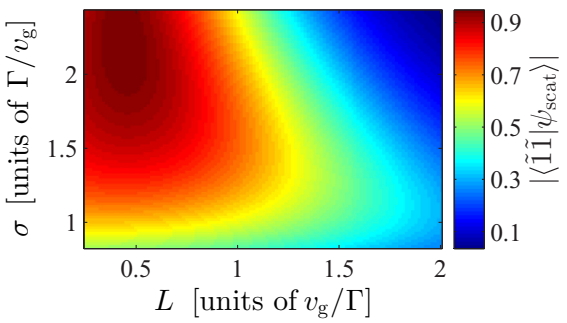

FIG. 4. Overlap between the ideal and scattered state for the $|1_c\rangle|1_s\rangle$ input as a function of the additional optical length of the 0 arms, L, and the input pulse width σ.

linewidth. For spectrally broader photons for which $\xi(k)$ extends beyond $k \sim \tilde{\Gamma}$, terms of higher order in k will have an influence and introduce chirping effects [19,20].

To illustrate this in more detail for a specific case, let us consider a Gaussian single-photon wave packet, defined by the spectral profile

$$\xi(k) = (\pi\sigma'^2)^{-1/4}\exp[-k^2/(2\sigma'^2)], \tag{9}$$

where the spectral bandwidth (FWHM of the intensity spectrum) is $\sigma = 2\sqrt{\ln(2)}\sigma'$. Figure 3 plots the magnitude of the overlap between the desired (ideal) state and actual state for a Gaussian spectrum as described above. As expected, the overlap increases when the spectral width σ is decreased. The optimum additional path length L approaches $L = 2v_g/\Gamma$ as σ is decreased, which is expected from the linear term in Eq. (8). For larger spectral widths, the optimum L decreases because a straight line with a slope smaller than $2v_g/\Gamma$ approximates the phase $\theta(k)$ better in this case, as seen in Fig. 2.

IV. NONLINEAR GATE INTERACTIONS

The nonlinear interaction occurs for the input state $|1_c\rangle|1_s\rangle$, where two photons may be present at the scatterers simultaneously, introducing nonlinear interactions through a two-photon bound state [37]. The nonlinear scattering is treated by the scattering matrix formalism following Ref. [37], and we include the directional coupler when calculating the scattered state of the entire gate. The gate input consists of two uncorrelated identical photons which we describe by

$$|\psi_{in}\rangle = \int_{-\infty}^{\infty}\int_{-\infty}^{\infty} dkdk'\xi(k)\xi(k')a_{c1}^{\dagger}(k)a_{s1}^{\dagger}(k')|\phi\rangle, \tag{10}$$

where as before $\int_{-\infty}^{\infty} dk|\xi(k)|^2 = 1$ to ensure that $|\psi_{in}\rangle$ contains two photons. Following the action of the first directional coupler, scattering on the two-level emitters, and passing through the second directional coupler, we find $|\psi_{in}\rangle \rightarrow |\psi_{scat}\rangle$ with the total scattered state given by

$$|\psi_{scat}\rangle = \int_{-\infty}^{\infty}\int_{-\infty}^{\infty} dkdk'\beta_{scat}(k,k')a_{c1}^{\dagger}(k)a_{s1}^{\dagger}(k')|\phi\rangle, \tag{11}$$

where we have removed a factor of $(-i)^2$ to be consistent with our definitions of the output states, and

$$\beta_{scat}(k,k') = \beta_{scat}^{linear}(k,k') + \tfrac{1}{2}b(k,k'), \tag{12}$$

with the linear contribution given by $\beta_{scat}^{linear}(k,k') = t(k)t(k')\xi(k)\xi(k')$ and a nonlinear scattering contribution by

$$b(k,k') = \int_{-\infty}^{\infty} dp\ \xi(p)\xi(k+k'-p)B_{kk'p(k+k'-p)}. \tag{13}$$

The scatterer-dependent coefficient $B_{kk'pp'}$ is evaluated in Ref. [49] for a two-level system,

$$B_{kk'pp'} = i\frac{\sqrt{2\Gamma/v_g}}{\pi}s(k)s(k')[s(p)+s(p')], \tag{14}$$

where

$$s(k) = \frac{\sqrt{2\Gamma/v_g}}{k-\Delta+i(\Gamma+\gamma)/(v_g)}. \tag{15}$$

The ideal output state in the nonlinear case is

$$|\tilde{1}_c\rangle|\tilde{1}_s\rangle = -\int_{-\infty}^{\infty}\int_{-\infty}^{\infty} dkdk'e^{i(k+k')L}a_{c1}^{\dagger}(k)a_{s1}^{\dagger}(k')|\phi\rangle, \tag{16}$$

where the minus sign accounts for the required phase flip that defines the controlled-PHASE gate.

To gain some insight into how well the actual state $|\psi_{scat}\rangle$ approximates the ideal state in Eq. (16), we plot the magnitude of their overlap as a function of L and σ in Fig. 4, again for Gaussian input pulses. In contrast to the one-photon-scattering case in Fig. 3, we now see that the largest overlap is observed for pulse widths $\sigma \approx 2.2\Gamma/v_g$. This is because it is for these widths that the nonlinearities are strongest and the required π phase shift can be generated, consistent with the results in Ref. [20].[1] Furthermore, the optimal value of L in this nonlinear-scattering case is significantly lower than in the linear case. A comparison of Figs. 3 and 4 demonstrates that limitations in the gate performance are expected to occur because of these different requirements on σ and L to optimally approximate the ideal output states in the linear and nonlinear cases, which we now explore in more detail.

[1] In Ref. [20], the interaction is reported strongest when $\sigma \sim \Gamma/v_g$. This occurs for an emitter in a bidirectional waveguide, which effectively has a decay rate twice as large as for the single-directional problem considered in this work. Thus, when projected onto this work, the strongest nonlinearity is expected around $\sigma \sim 2\Gamma/v_g$.

V. FIDELITY OF GATE OPERATION

To find the optimal spectral width σ and path length difference L, we now consider the operation of the gate as a whole. When incorporated into a larger optical circuit, the logical input state of the gate will necessarily be unknown, and the gate must therefore be able to operate for any linear combination of the four possible logical input states. As such, the gate performance must be quantified by a fidelity based on a worst-case scenario, in which the output state of the gate is compared with the ideal target output state, minimized over all possible input states. A gate fidelity meeting these requirements is defined as [50]

$$F(\hat{U},\hat{\mathcal{E}}) \equiv \min_{|\psi\rangle} F_s(\hat{U}|\Psi\rangle\langle\Psi|\hat{U}^\dagger,\hat{\mathcal{E}}(|\Psi\rangle\langle\Psi|)), \tag{17}$$

where $\hat{U}$ and $\hat{\mathcal{E}}$ describe the transformations of the ideal and actual gate, respectively, and F_s is the state fidelity defined by [50]

$$F_s(\hat{\rho},\hat{\sigma}) \equiv \mathrm{Tr}\Big\{\sqrt{\hat{\rho}^{\frac{1}{2}}\hat{\sigma}\hat{\rho}^{\frac{1}{2}}}\Big\}, \tag{18}$$

for two density operators, $\hat{\rho}$ and $\hat{\sigma}$. The arbitrary input state $|\Psi\rangle$ is given by

$$\begin{aligned}|\Psi\rangle &= (\alpha|0_s\rangle + \beta|1_s\rangle) \otimes (\zeta|0_c\rangle + \vartheta|1_c\rangle)\\ &= \alpha\zeta|00\rangle + \alpha\vartheta|01\rangle + \beta\zeta|10\rangle + \beta\vartheta|11\rangle,\end{aligned} \tag{19}$$

where $|0_s\rangle|0_c\rangle \equiv |00\rangle$, etc. Using the definitions from previous sections, the ideal gate transformation is

$$\hat{U}|\Psi\rangle = \alpha\zeta|\tilde{0}\tilde{0}\rangle + \alpha\vartheta|\tilde{0}\tilde{1}\rangle + \beta\zeta|\tilde{1}\tilde{0}\rangle - \beta\vartheta|\tilde{1}\tilde{1}\rangle. \tag{20}$$

If we neglect loss, the output states are pure and the actual (possibly imperfect) transformation is described by $\hat{\mathcal{E}}(|\Psi\rangle\langle\Psi|) = \hat{T}|\Psi\rangle\langle\Psi|\hat{T}^\dagger$, with

$$\hat{T}|\Psi\rangle = \alpha\zeta|\tilde{0}\tilde{0}\rangle + \alpha\vartheta|\tilde{0}\tilde{1}\rangle + \beta\zeta|\tilde{1}\tilde{0}\rangle + \beta\vartheta|\psi_{\mathrm{scat}}\rangle, \tag{21}$$

where $|\psi_{\mathrm{scat}}\rangle$ is given by Eq. (11). For pure states, Eq. (18) simplifies to $F_s(|a\rangle\langle a|,|b\rangle\langle b|) = |\langle a|b\rangle|$, and the state fidelity is therefore

$$\begin{aligned}&F_s(\hat{U}|\Psi\rangle\langle\Psi|\hat{U}^\dagger,\hat{T}|\Psi\rangle\langle\Psi|\hat{T}^\dagger)\\ &\quad= |\langle\Psi|\hat{U}^\dagger\hat{T}|\Psi\rangle|\\ &\quad= ||\alpha\zeta|^2 + \langle\tilde{1}|\tilde{1}\rangle(|\alpha\vartheta|^2 + |\beta\zeta|^2) - |\beta\vartheta|^2\langle\tilde{1}\tilde{1}|\psi_{\mathrm{scat}}\rangle|.\end{aligned} \tag{22}$$

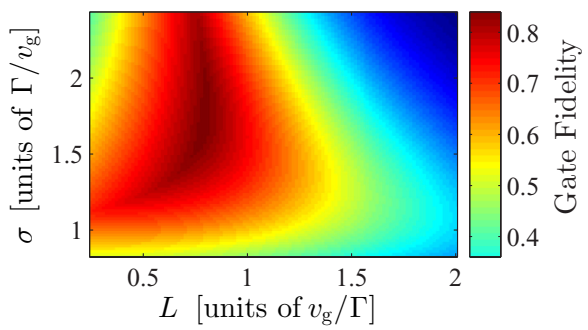

FIG. 5. Gate fidelity as a function of the additional optical length of the 0 arms, L, and the input pulse width σ.

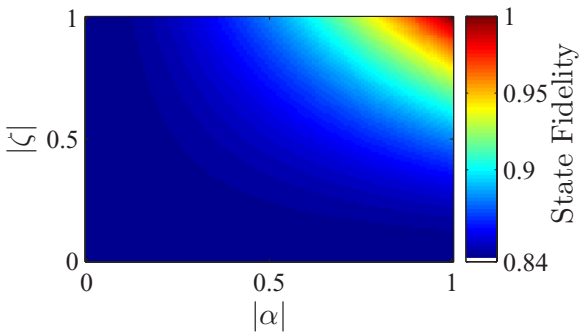

FIG. 6. State fidelity as a function of input states expressed by $|\alpha|$ and $|\zeta|$ for $L = 0.80v_g/\Gamma$ and $\sigma = 1.72\Gamma/v_g$ corresponding to the maximum gate fidelity in Fig. 5.

To find the fidelity of the gate for a given pulse width and path length difference, this state fidelity must be minimized over all possible logical input states $|\Psi\rangle$ parameterized by the coefficients α, β, ζ, ϑ. Since the state fidelity only depends on the magnitude of the coefficients and the signal and control input states both must be normalized, the minimization in Eq. (17) can be carried out by varying only, e.g., $|\alpha|$ and $|\zeta|$. By performing this minimization for different values of σ and L, the trade-offs due to the effects of linear and nonlinear scattering can be quantified. The result is shown in Fig. 5, where the gate fidelity is plotted as a function of L and σ, again for Gaussian pulses. The optimum set of parameters is seen to be close to that in Fig. 4 but shifted towards smaller pulse widths and larger L, where the optimum was observed in Fig. 3. This trend is expected, since Eq. (22) effectively performs a weighted average of the overlaps in Figs. 3 and 4.

To confirm that the gate fidelity indeed corresponds to a worse-case scenario, Fig. 6 shows the dependence of the state fidelity on the input states for the optimum parameter set in Fig. 5. It shows that the state fidelity approaches unity for the state $|0_c\rangle|0_s\rangle$, and is above 84% for the entire state space, as expected.

Finally, we note that our formalism easily allows for spectra other than Gaussians to be considered. Most notably, we find that Lorentzian spectral profiles result in a worse gate fidelity of $F \approx 62\%$. Although a Lorentzian-shaped single-photon is expected to most efficiently populate a two-level emitter, two such coincident pulses give rise to a smaller induced nonlinearity [19], which is an essential requirement for the gate to operate. We find that sech^2 pulses achieve a fidelity marginally better than Gaussian pulses, raising the gate fidelity by only 0.5%. Ultimately active modification of spectra may be necessary if gates based on two-level-emitter nonlinearities are to attain fidelities approaching unity [35].

VI. CONCLUSION

We have investigated in detail the feasibility of using two-level-emitter nonlinearities to construct a passive two-photon controlled-PHASE gate, elucidating the nonlinearity-induced changes in the spectrum. We find that these effects ultimately limit the fidelity of a controlled-PHASE gate based on two-level-emitter nonlinearities, giving $F \approx 84\%$ for Gaussian input pulses, decreasing to $F \approx 62\%$ for Lorentzian spectra. We

emphasize, however, that the scheme we consider requires no dynamical capture of photons [34], uses only two identical two-level emitters, and does not make use of pulse reshaping techniques. Although schemes making use of multiple nonlinearities per gate [36], or gradient echo memory [35] to reverse pulse shapes, predict theoretical fidelities approaching unity, these processes increase the complexity of the gate and are likely to introduce additional losses. Ultimately it seems likely that efficiency-fidelity trade-offs will be present in any gate scheme, and these trade-offs must be carefully considered in a larger photonic network with a given application.

ACKNOWLEDGMENTS

A.N. and J.M. acknowledge support from Villum Fonden via the NATEC Centre (Grant No. 8692). M.H. acknowledges support from DFF:1325-00144. D.R.E. acknowledges support from AFOSR MURI for Optimal Measurements for Scalable Quantum Technologies (FA9550-14-1-0052) and the Air Force Research Laboratory RITA program (FA8750-14-2-0120). This project has received funding from the European Union's Horizon 2020 research and innovation programme under the Marie Skłodowska-Curie Grant Agreement No. 703193.

[1] E. Knill, R. Laflamme, and G. J. Milburn, Nature (London) **409**, 46 (2001).
[2] P. Kok, W. J. Munro, K. Nemoto, T. C. Ralph, J. P. Dowling, and G. J. Milburn, Rev. Mod. Phys. **79**, 135 (2007).
[3] P. Kok and B. W. Lovett, *Introduction to Optical Quantum Information Processing* (Cambridge University Press, Cambridge, 2010).
[4] T. C. Ralph, N. K. Langford, T. B. Bell, and A. G. White, Phys. Rev. A **65**, 062324 (2002).
[5] M. A. Pooley, D. J. P. Ellis, R. B. Patel, A. J. Bennett, K. H. A. Chan, I. Farrer, D. A. Ritchie, and A. J. Shields, Appl. Phys. Lett. **100**, 211103 (2012).
[6] M. Gimeno-Segovia, P. Shadbolt, D. E. Browne, and T. Rudolph, Phys. Rev. Lett. **115**, 020502 (2015).
[7] J. L. O'Brien, G. J. Pryde, A. G. White, T. C. Ralph, and D. Branning, Nature (London) **426**, 264 (2003).
[8] A. Kuhn, M. Hennrich, and G. Rempe, Phys. Rev. Lett. **89**, 067901 (2002).
[9] M. Hijlkema, B. Weber, H. P. Specht, S. C. Webster, A. Kuhn, and G. Rempe, Nature (London) **3**, 253 (2007).
[10] I. Aharonovich, D. Englund, and M. Toth, Nat. Photon. **10**, 631 (2016).
[11] N. Somaschi *et al.*, Nat. Photon. **10**, 340 (2016).
[12] X. Ding, Y. He, Z. C. Duan, N. Gregersen, M. C. Chen, S. Unsleber, S. Maier, C. Schneider, M. Kamp, S. Höfling *et al.*, Phys. Rev. Lett. **116**, 020401 (2016).
[13] J. Iles-Smith, D. P. S. McCutcheon, A. Nazir, and J. Mørk, arXiv:1612.04173.
[14] I. L. Chuang and Y. Yamamoto, Phys. Rev. A **52**, 3489 (1995).
[15] L. M. Duan and H. J. Kimble, Phys. Rev. Lett. **92**, 127902 (2004).
[16] S. Das, A. Grankin, I. Iakoupov, E. Brion, J. Borregaard, R. Boddeda, I. Usmani, A. Ourjoumtsev, P. Grangier, and A. S. Sørensen, Phys. Rev. A **93**, 040303 (2016).
[17] B. Hacker, S. Welte, G. Rempe, and S. Ritter, Nature (London) **536**, 193 (2016).
[18] A. Auffèves-Garnier, C. Simon, J.-M. Gérard, and J.-P. Poizat, Phys. Rev. A **75**, 053823 (2007).
[19] A. Nysteen, D. P. S. McCutcheon, and J. Mørk, Phys. Rev. A **91**, 063823 (2015).
[20] A. Nysteen, P. T. Kristensen, D. P. S. McCutcheon, P. Kaer, and J. Mørk, New J. Phys. **17**, 023030 (2015).
[21] Z. Zhao, A.-N. Zhang, Y.-A. Chen, H. Zhang, J.-F. Du, T. Yang, and J.-W. Pan, Phys. Rev. Lett. **94**, 030501 (2005).
[22] S. Gasparoni, J.-W. Pan, P. Walther, T. Rudolph, and A. Zeilinger, Phys. Rev. Lett. **93**, 020504 (2004).
[23] A. Crespi, R. Ramponi, R. Osellame, L. Sansoni, I. Bongioanni, F. Sciarrino, G. Vallone, and P. Mataloni, Nat. Commun. **2**, 566 (2011).
[24] A. Reiserer, N. Kalb, G. Rempe, and S. Ritter, Nature (London) **508**, 237 (2014).
[25] I. Shomroni, S. Rosenblum, Y. Lovsky, O. Bechler, G. Guendelman, and B. Dayan, Science **345**, 903 (2014).
[26] T. G. Tiecke, J. D. Thompson, N. P. de Leon, L. R. Liu, V. Vuletic, and M. D. Lukin, Nature (London) **508**, 241 (2014).
[27] H. Kim, R. Bose, T. C. Shen, G. S. Solomon, and E. Waks, Nat. Photon. **7**, 373 (2013).
[28] T. Volz, A. Reinhard, M. Winger, A. Badolato, K. J. Hennessy, E. L. Hu, and A. Imamoğlu, Nat. Photon. **6**, 605 (2012).
[29] D. Englund, A. Majumdar, M. Bajcsy, A. Faraon, P. Petroff, and J. Vučković, Phys. Rev. Lett. **108**, 093604 (2012).
[30] R. Bose, D. Sridharan, H. Kim, G. S. Solomon, and E. Waks, Phys. Rev. Lett. **108**, 227402 (2012).
[31] C. Wang, Y. Zhang, R.-Z. Jiao, and G.-S. Jin, Opt. Express **21**, 19252 (2013).
[32] K. Koshino, S. Ishizaka, and Y. Nakamura, Phys. Rev. A **82**, 010301 (2010).
[33] C. Chudzicki, I. L. Chuang, and J. H. Shapiro, Phys. Rev. A **87**, 042325 (2013).
[34] R. Johne and A. Fiore, Phys. Rev. A **86**, 063815 (2012).
[35] T. C. Ralph, I. Söllner, S. Mahmoodian, A. G. White, and P. Lodahl, Phys. Rev. Lett. **114**, 173603 (2015).
[36] D. J. Brod and J. Combes, Phys. Rev. Lett. **117**, 080502 (2016).
[37] S. Fan, Ş. E. Kocabaş, and J.-T. Shen, Phys. Rev. A **82**, 063821 (2010).
[38] S. Xu, E. Rephaeli, and S. Fan, Phys. Rev. Lett. **111**, 223602 (2013).
[39] J. H. Shapiro, Phys. Rev. A **73**, 062305 (2006).
[40] D. Witthaut, M. D. Lukin, and A. S. Sørensen, Europhys. Lett. **97**, 50007 (2012).
[41] A. Biberman, M. J. Shaw, E. Timurdogan, J. B. Wright, and M. R. Watts, Opt. Lett. **37**, 4236 (2012).
[42] H. Sekoguchi, Y. Takahashi, T. Asano, and S. Noda, Opt. Express **22**, 916 (2014).
[43] Y.-Z. Sun, Y.-P. Huang, and P. Kumar, Phys. Rev. Lett. **110**, 223901 (2013).
[44] M. G. Thompson, A. Politi, J. C. F. Matthews, and J. L. O'Brien, IET Circuits, Devices Syst. **5**, 94 (2011).
[45] J. Wang, A. Santamato, P. Jiang, D. Bonneau, E. Engin, J. W. Silverstone, M. Lermer, J. Beetz, M. Kamp, S. Höfling *et al.*, Opt. Commun. **327**, 49 (2014).

[46] A. Martinez, F. Cuesta, and J. Marti, IEEE Photon. Technol. Lett. **15**, 694 (2003).

[47] N. C. Harris, D. Bunandar, M. Pant, G. R. Steinbrecher, J. Mower, M. Prahbu, T. Baehr-Jones, M. Hochberg, and D. Englund, Nanophotonics **5**, 456 (2016).

[48] J.-T. Shen and S. Fan, Phys. Rev. A **76**, 062709 (2007).

[49] E. Rephaeli and S. Fan, Photonics Res. **1**, 110 (2013).

[50] M. A. Nielsen and I. L. Chuang, *Quantum Computation and Quantum Information* (Cambridge University Press, 2000).